Annals of University of Craiova, Math. Comp. Sci. Ser.
Volume 30(1), 2006, Pages 44–53
ISSN: 1223-6934

Particle-based Magnetohydrodynamics Modeling and Visualization: Part II - Numerical Simulation

Mihai Dupac

Abstract. In this paper a particle-base model is used to visualize results of the magnetohydrodynamics (MHD) phenomena related to electromagnetic levitation (EML) and magnetic stirring. Using the theoretical model presented in Part I, a numerical algorithm for fluid flow simulation has been described. To struggle out the local dynamics, the position and velocity of each particle is visualized and the interface is reconstructed. The model was verified for both cases, EML and magnetic stirring.

2000 Mathematics Subject Classification. Primary 60J05; Secondary 60J20.
Key words and phrases. particle method, magnetohydrodynamics, flow visualization, vector field visualization.

1. Introduction

Visualization techniques are indispensable tools for the understanding of dynamical systems such as computational fluid dynamics (CFD) or MHD. The visualization of the 3D flow phenomena, especially of velocity field from CFD computations is one of the fundamental tasks in scientific visualization and a challenging subject in order to interpret the data and to have a better understanding of complex flow phenomena.

Several visualization techniques for two-dimensional and three-dimensional flows have already been investigated. Some examples of flow visualization techniques, ranging from streamlines to texture based techniques, i.e., Line Integral Convolution (LIC) and variations of the LIC, are described in [4, 7]. A general streamline placement was introduced in [16], and a refined technique for creating evenly-spaced streamlines in [8].

Visualization of time-dependent phenomena, such as three-dimensional turbulent flows or unsteady flows based on particle tracking was discussed in [10]. Visualization of time-varying fluid flows using large amounts of particles has been studied in [11]. Other particles approach for visualizing three-dimensional fluid flows near surface vicinity, with particle generation and deletion density based, are presented in [12].

Real time rendering of large amounts of particles and fluid interface particle tracing algorithms have been developed for different types of meshes in [13] and [17] respectively. A different approach for small particle systems was used in [5].

The work in the present paper is dedicated to visualize the fluid flow phenomena using particles in a mesh-free approach. Following the theoretical model described in Part I, a numerical algorithm for fluid flow simulation, obtained using the Moving-Particle Semi-implicit (MPS) method [9, 14, 15] has been described.

Furthermore to struggle out the local dynamics, the position and velocity of each particle is computed and continuously updated. Results from the simulation for the

Received: 11 December 2002.

case of EML (levitated droplet) and electromagnetic stirring (rotating cylindrical sample) are presented. The droplet was analyzed in a force field, which is derived from the magnetic field produced by the coil. The cylinder was analyzed in a constant magnetic field. The electromagnetic force distribution and velocity field were computed and visualized. Three-dimensional numerical analysis of the effect of the surface oscillations for a levitated (EML) droplet are carried out.

The advantage of the presented numerical method (mesh-free method) is that enables accurate three-dimensional flow modeling, simplifies the calculation of the interface, and does not impose any modeling restrictions on the dynamic evolution of fluid interfaces having surface tension. It is also a good method for the study of the surface deformation and the design of the EML or magnetic stirring process.

2. Numerical Algorithm

To simulate the MHD phenomena using particles, the continuous time is discretized into time steps and then the Navier-Stokes equations of motion are solved numerically. For every time step Δt, the forces in the momentum equation are computed explicitly as follows:

1. The right hand side of Navier-Stokes equation is solved explicitly and the temporal velocity is computed.
2. The temporal particle location of the particles are updated.
3. The pressure is computed implicitly using Poisson's equation
4. A new temporal velocity is updated using the pressure gradient
5. A new temporal particle location is updated using the new temporal velocity
6. Check for convergence using an error limit based on the size of the difference between Step 4 and Step 5

6.1. If *not converging* go back to Step 3.
6.2. If *converging* return to Step 1.

Algorithm

1. $\mathbf{u}^* \leftarrow \mathbf{u}^n + \dfrac{\Delta t}{\rho}\left(\eta\nabla^2\mathbf{u}^n + \mathbf{F}_g + \mathbf{F}_{el}^n + \mathbf{F}_{st}^n\right)$

2. $\mathbf{r}^* \leftarrow \mathbf{r}^n + \mathbf{u}^*\Delta t$

3. $\nabla^2 p^{n+1} \leftarrow -\dfrac{\rho}{\Delta t}\nabla\cdot\mathbf{u}^*$

4. $\mathbf{u}' \leftarrow \mathbf{u}^* - \dfrac{\Delta t}{\rho}\nabla p^{n+1}$

5. $\mathbf{r}' \leftarrow \mathbf{r}^* + \mathbf{u}'\Delta t$

6. Check for convergence

6.1 $\mathbf{u}^{n+1} \leftarrow \mathbf{u}'$

6.2 $\mathbf{r}^{n+1} \leftarrow \mathbf{r}'$

In the previous algorithm $\mathbf{u}^*$ is the temporal velocity, the superscript "n" refers to the n^{th} time step, Δt is the step size, η is the viscosity of the fluid, $\mathbf{F}_g = \rho\mathbf{g}$ represents the gravity force, ρ is the density, $\mathbf{F}_{el}^n = \mathbf{F}^n$ represents the electromagnetic force density computed for each particle of the droplet, $\mathbf{F}_{st}^n = \sigma\left(k\cdot\mathbf{n}\right)^n$ is the surface tension force, σ is the surface tension coefficient, k is the mean curvature of the interface, δ is the Dirac delta function that is zero everywhere except at the interface, $\mathbf{n}$ is the unit normal vector to the interface, $\mathbf{r}^*$ is the temporal particle location, $\mathbf{r}^n$ represents the positions from the previous time step, $\mathbf{u}'$ is the new temporal velocity

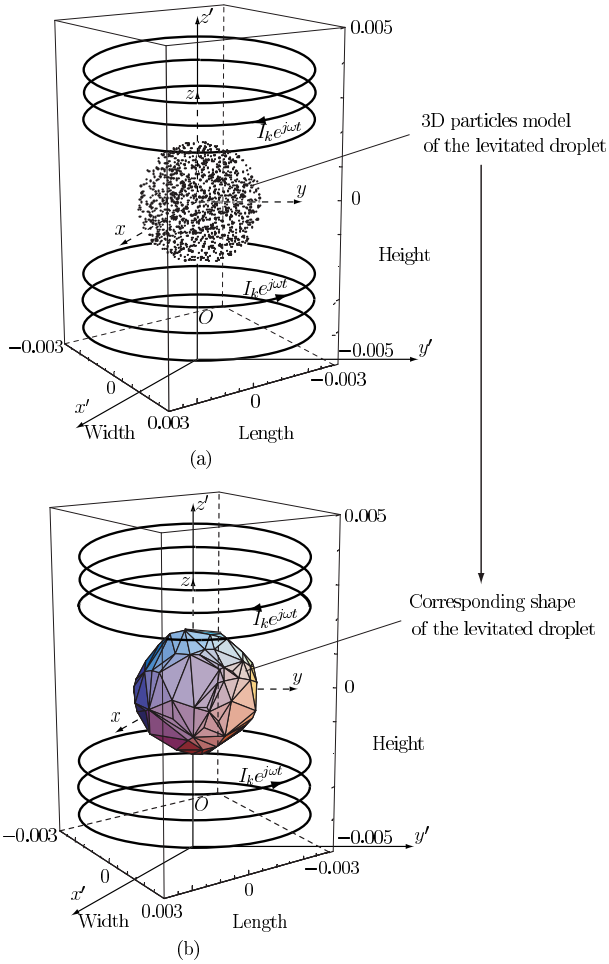

FIGURE 1. (a) 3D Particles Model of the Levitated Aluminum Droplet, and, (b) Shape of the Levitated Aluminum Droplet

updated using the pressure gradient and $\mathbf{r}'$ is the new temporal particle location updated using the new temporal velocity.

3. Implementation and Results

Results from the simulation of a levitated aluminum droplet by two parallel loops carrying electric currents in opposed direction, and from the simulation of a rotating cylindrical aluminum sample in a constant magnetic field, are presented. The droplet is analyzed in a force field, which is derived from the magnetic field produced by the coil. The cylindrical sample is analyzed in a constant magnetic field. The levitation coil and the aluminum sample modeled as a 3D particle system are shown in Fig. 1.a. The corresponding shape of the levitated droplet is shown in Fig. 1.b. The rotating cylinder modeled as a 3D particle system is shown in Fig. 2. The initial temperature of the sample (droplet and cylindrical sample) was considered to be 750° C. A 3D particles system model, with a number of 600 particles (Fig. 1.a) were considered

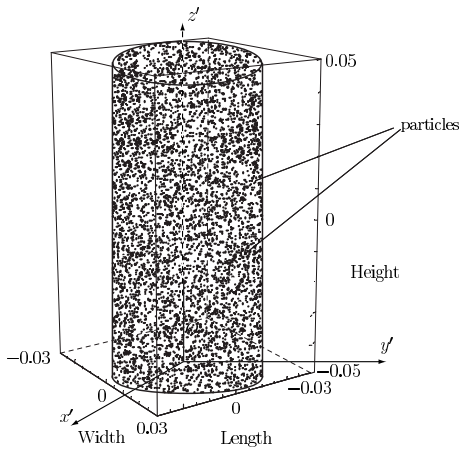

FIGURE 2. 3D Particles Model of the Rotating Cylindrical Aluminum Sample

for the analysis of the levitated droplet. A number of 7500 particles (Fig. 2) were considered for the analysis of the rotating cylindrical sample. The behavior of the aluminum specimens (levitated aluminum droplet and cylindrical aluminum sample) was studied using the next system parameters.

Parameters	Symbol	Value	Units
Density	ρ	2700	$\mathrm{Kg/m^3}$
Electro − Conductivity	σ_c	3.9×10^6	$(\Omega - \mathrm{m})^{-1}$
Current	I	500	A
Frequency	f	300	kHz
Magnetic Permeability	μ	$4\pi \times 10^{-7}$	H/m
Viscosity	η	1.3×10^{-3}	m
Volume Expansion Coefficient	β	1.15×10^{-4}	1/K
Gravity	g	9.81	$\mathrm{m/s^2}$
Droplet Radius	R	2.5×10^{-3}	m
Cylindrical Sample Radius	r	2.75×10^{-2}	m
Cylindrical Sample Height	h	10.0×10^{-2}	m

Table 1

The volume electromagnetic forces distribution acting on each particle have been continuously computed and updated. The computation was made by neglecting the diffusion of the magnetic field during the motion and under the assumption that the induced magnetic field is negligible compared with the imposed field.

The electromagnetic forces distribution, for the case of the levitated aluminum droplet, exerted on each particle of the system, was plotted in Fig. 3.a. As seen from Fig. 3.a, the force distribution is highly non-uniform. The electromagnetic forces distribution, for the case of the rotating cylindrical sample, exerted on each particle of the system, was plotted in Fig. 3.b.

For the electromagnetic case, the simulation show that the electromagnetic force density introduced a circulation with a very small velocity (10^{-2} m/sec) as shown in Fig. 4.a. As seen from Fig. 3.a, the turbulent viscosity (as indicated by the almost random force direction) is mainly generated in the bottom part of the levitated droplet

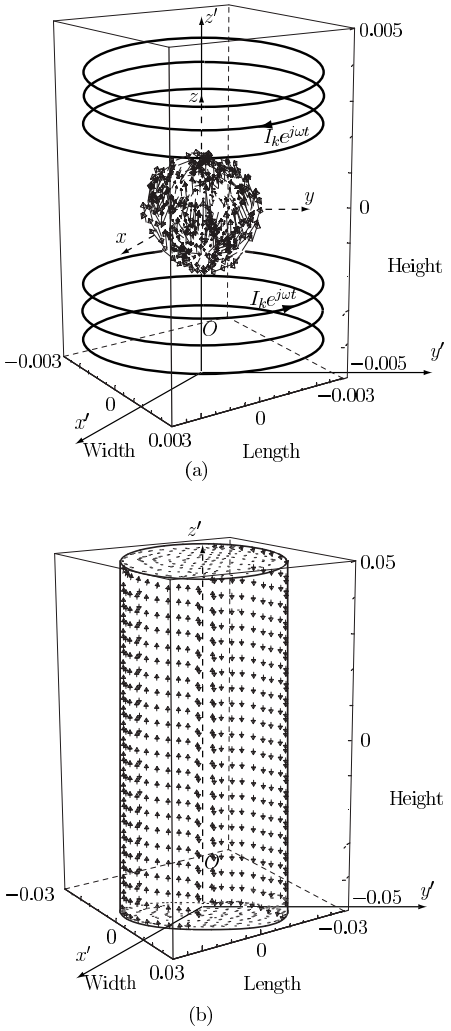

FIGURE 3. Electromagnetic Force Distribution of the (a) Levitated Aluminum Droplet, and, (b) Rotating Cylindrical Aluminum Sample. The Figure uses arrows with a 3-D tip to show the direction

and then transported to the rest of the volume. The velocity field of the rotating cylinder is shown in Fig. 4.b.

Under terrestrial levitation conditions, the aluminum droplet is distorted from its spherical shape owing to the existence of the magnetic field and gravity. Using the numerical algorithm and a surface tension coefficient, $s = 0.86$ N/m, reported by [1], the shape changes of a levitated droplet are simulated and the coordinates of the center of mass, the surface shape and the radius of the droplet (three perpendicular diameters in the vertical, horizontal and transversal directions and their dependence on time) have been determined.

At the beginning of the simulation the levitated droplet has been assumed to have a spherical shape. Then, the molten sample was excited about 4 seconds. From Fig. 5 it can be observed that a initial transient time (first $2.2 - 2.3$ seconds of the

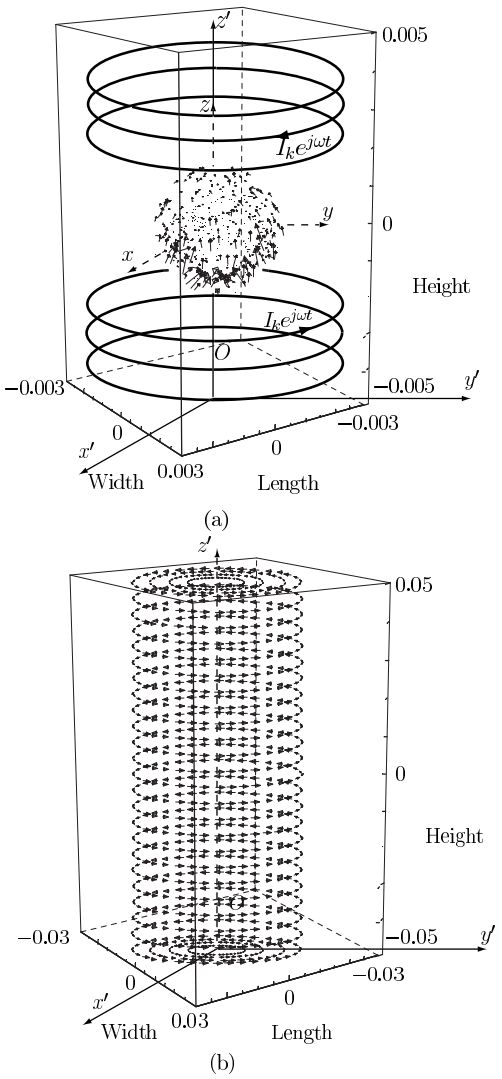

FIGURE 4. Velocity Field of the (a) Levitated Aluminum Droplet, and, (b) Rotation Cylindrical Aluminum Sample

simulation) occurred, during which the levitated sample assumes the shape imposed by the levitated force. In the numerical calculation, the oscillations damp after some time (first $2.2 - 2.3$ seconds of the simulation). The decay of the oscillations can be clearly visualized in the droplet oscillations shown in Fig. 5.

To analyze the surface oscillation, data for the change in the radius of the droplet were input into a fast Fourier transformation (FFT). From the FFT, the frequency spectra of the surface oscillations has been obtained as shown in Fig. 6.

Since a numerical algorithm has been used, the surface oscillations can be analyzed in more detail. Fourier analysis reveals 2 principal peaks in the frequency spectrum, which corresponds to the 2 dominant frequencies of the specimen under normal gravity conditions. As it can be observed from the fast Fourier transform, the levitated

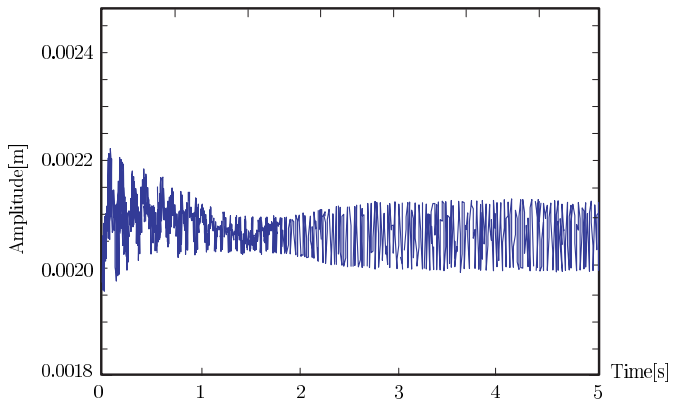

FIGURE 5. Aluminum Droplet Oscillations Simulated in Normal Gravity, as Measured by Change in Vertical Radius

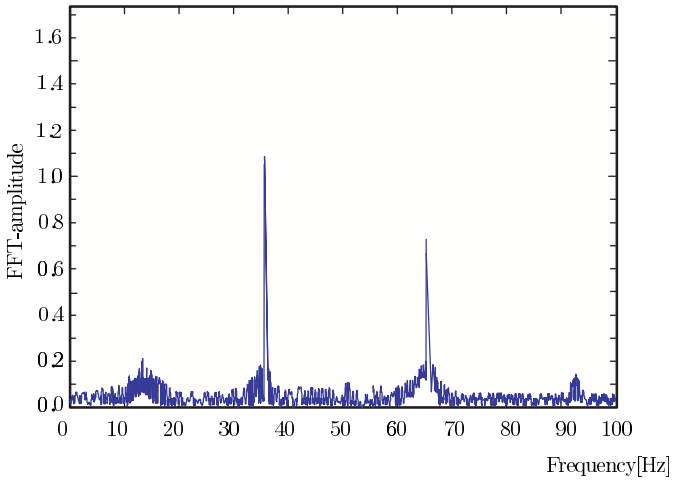

FIGURE 6. Fourier Power Spectra of the vertical Radius for the Aluminum Droplet Oscillations

aluminum specimen leads to a dominant frequency of 35.97 Hz and a secondary frequency of 64.73 Hz. The dominant frequency corresponds closely to the 35.39 Hz (Rayleigh formula) of the 2^{nd} mode. The secondary frequency is very close to the 3^{rd} theoretical mode frequency at 68.42 Hz (Rayleigh formula). Also, a translational motion frequency at 12.76 Hz relatively close to the 1^{st} theoretical mode frequency has been observed.

The obtained results are in good agrement with the analysis shown in [6]. It was observed that the 1^{st} mode of oscillation of a levitated specimen corresponds to the translational motion of the specimen, whereas the other modes are related to its surface oscillation. The numerical computation relates an oscillation frequency with the appropriate oscillation mode by comparison of different frequency spectra. The geometry of the oscillations for 2^{nd} mode is shown in Fig. 8 and for the 1^{st} mode corresponding to the translational motion of the specimen, in Fig. 7.

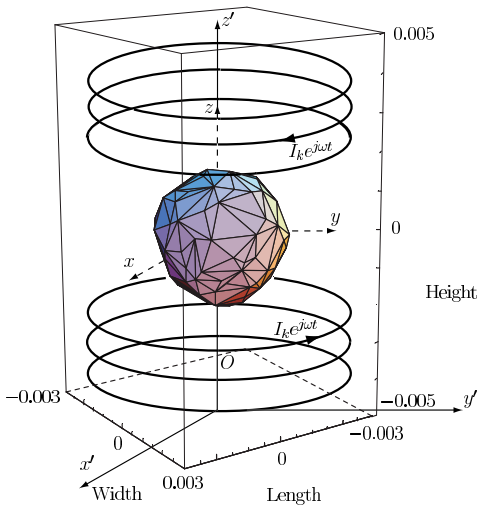

FIGURE 7. Geometry of the Translational Oscillation Mode of the Aluminum Sample

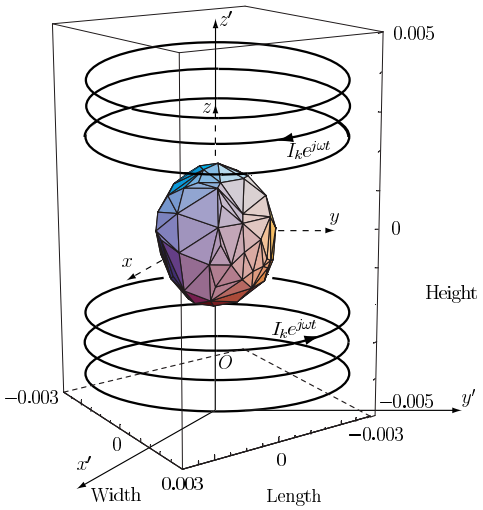

FIGURE 8. Geometry of the 2^{nd} Oscillation Mode of the Aluminum Sample

The obtained numerical results were compared with other reported results (theoretical and/or experimental) found in literature, and a very good agreement (with respect to the overall systematic error quoted to be the sample variance) was observed.

4. Conclusions

In this paper a particle-base model numerical simulations is used to visualize results of MHD phenomena related to EML (levitated droplet) and magnetic stirring (rotating cylindrical sample), subjected to a electromagnetic and external forces.

A mesh-free numerical algorithm based on a theoretical model (MPS method) described in Part I has been used for fluid flow simulation. Different time-dependent phenomena, such as three-dimensional unsteady flows, velocity field, electromagnetic force distribution or shape changes/surface deformations/surface oscillations, has been visualized.

Excellent agreement was found between the obtained numerical results and other reported results found in literature.

References

[1] J. P. Anson, R.A.L. Drew, and J.E. Gruzeleski, The Surface Tension of Molten Aluminum and Al-Si-Mg Alloy under Vacuum and Hydrogen Atmospheres, *Metallurgical and Materials Transactions,* **30**, 1027-1034, (1999).

[2] J.U. Brackbill, D.B. Kothe and C. Zemach, A continuum method for modeling surface tension, *Journal of Computational Physics,* **100**, pp. 335-354, (1992).

[3] F.H. Busse, Oscillations of a Rotating Liquid Drop, Journal of Fluid Mechanics, **142**, 1-8, (1984).

[4] B. Cabral, and L.C. Leedom, Imaging Vector Fields using line Integral Convolution. In *Proceedings of ACMSIGGRAPH 93, Computer Graphics Proceedings, Annual Conference Series*, 263-272, (1993).

[5] M.B. Cox and D. Ellsworth, Application-controlled demand paging for Out-of-Core visualization, in *IEEE Visualization 97, Roni Yagel and Hans Hagen, Eds., Los Alamitos, California, USA, IEEE Computer Society Press*, 235-244, (1997).

[6] D.L. Cummings, and D.A. Blackburn, Oscillations of Magnetically Levitated Aspherical Droplets, *Journal of Fluid Mechanics*, **224**, 395-416, (1989).

[7] W. Heidrich, R. Westermann, H.-P. Seidel, and T. Ertl, Applications of Pixel Textures in Visualization and Realistic Image Synthesis, In *ACM Symposium on Interactive 3D Graphics*, 127134, (1999).

[8] B. Jobard and W. Lefer, Creating Evenly Spaced Streamlines of Arbitrary Density, In *Wilfrid Lefer and Michel Grave, editors, Visualization in Scientific Computing, Springer-Wien-NewYork,* , 4355, (1997).

[9] S. Koshizuka, and Y. Oka, Numerical Analysis of Droplet Breakup Behavior using Particle Method, *Nucl. Sci. Eng*, **123**, 421-434, (1996).

[10] D.N. Kenwright and D.A. Lane, Optimization of timedependent particle tracing using tetrahedral decomposition. In Gregory M. Nielson and Deborah Silver, editors, Proceedings of Visualization 95, IEEE, 321-328, (1995).

[11] D.A. Lane, UFAT - A particle tracer for time dependent flow fields, In *in Proceedings of the Conference on Visualization, R. Daniel Bergeron and Arie E. Kaufman, Eds., Los Alamitos, California, USA, IEEE Computer Society Press.*, 257-264, (1994).

[12] N. Max, R. Crawfis, and C. Grant, Visualizing 3D Velocity Fields near Contour Surfaces. In IEEE Visualization 94 Proceedings, 248255, (1994).

[13] C. Meiselbach and R. Bruckschen, Interactive visualization: On the way to a virtual wind tunnel, in *Flow Simulation with High-Performance Computers, II, Ernst Heinrich Hirschel, Ed., of Notes on Numerical Fluid Mechanics, F. Vieweg and Sohn, Wiesbaden, Germany*, **52**, 203-208, (1996).

[14] K. Nomura, S. Koshizuka, Y. Oka, and H. Obata, Numerical Analysis of Droplet Breakup Behavior using Particle Method, *Journal of Nuclear Science and technology*, **38**(12), 1057-1064, (2001).

[15] S. Premoze, T. Tasdizen, J. Bigler, A. Lefohn, and R. T. Whitaker, Particle-Based Simulation of Fluids, *Eurographics*, **22**(3), (2003)

[16] G. Turk and D. Banks, Image-guided Streamline Placement, In *Proceedings SIGGRAPH 1996*, 453459, (1996).

[17] S.-K. Ueng, C. Sikorski, and K.-L. Ma, Out-of-core streamline visualization on large unstructured meshes, *IEEE Transactions on Visualization and Computer Graphics*, **3**(4), 370-380, (1997).

[18] H.Y. Yoon, S. Koshizuka, and Y. Oka, A Particle-Gridless Hybrid Method for incompressible Flows, *International Journal for Numerical Methods in Fluids*, **30**, 407-424, (1999).

(Mihai Dupac) Department of Informatics, University of Craiova,
Al.I. Cuza Street, No. 13, Craiova RO-200585, Romania, Tel. & Fax: 40-251412673
E-mail address: mihai.dupac@central.ucv.ro